Magnetic anisotropy and magnetic phase transitions in a $DyFe_{11}Ti$ single crystal

1994 J. Phys.: Condens. Matter 6 10551

(http://iopscience.iop.org/0953-8984/6/48/016)

J. Phys.: Condens. Matter 6 (1994) 10551–10566. Printed in the UK

Magnetic anisotropy and magnetic phase transitions in a $DyFe_{11}Ti$ single crystal

P A Algarabel, M R Ibarra, J Bartolomé, L M García and M D Kuz'min

Instituto de Ciencia de Materiales de Aragón and Departamento de Física de la Materia Condensada, Facultad de Ciencias, Consejo Superior de Investigaciones Científicas—Universidad de Zaragoza, 50009 Zaragoza, Spain

Received 24 June 1994, in final form 13 September 1994

Abstract. The magnetic anisotropy of the $DyFe_{11}Ti$ intermetallic has been studied by measuring the angular dependence of the components of the magnetization parallel and perpendicular to the applied magnetic field. The measurements were performed on two plate-shaped samples with the surfaces parallel to the $(\bar{1}10)$ and (001) planes, respectively. From the measurements in the $(\bar{1}10)$ plane the thermal dependence of the spin reorientation angle has been obtained. The magnetic field dependence of $M_{\parallel}$ and $M_{\perp}$ showed a first-order magnetization process (FOMP).

A single-ion model for the crystal-electric-field interaction and a mean-field model for the exchange interaction have been used to explain theoretically the experimental results.

An in-depth study of the character of the spin reorientation transition from easy cone to easy plane has been undertaken. From our study we show that for temperatures near this spin reorientation temperature, two magnetic phases (planar and conical phases) coexist in the sample, giving rise to an average angle that evolves continuously with temperature.

A similar behaviour has been also observed for magnetic fields near the critical field of the FOMP, producing a continuous change of the magnetization instead of a jump at the critical field.

1. Introduction

The basic magnetic properties of the $REFe_{12-x}M_x$ intermetallic compounds (RE = rare earth and M = Mo, Ti, Si, V, W or Cr) have been studied in depth during the last few years in view of their prospect as basis compounds for permanent magnet materials (see, for instance, Buschow *et al* 1989, Li and Coey 1991, Franse and Radwanski 1992). However, their performances cannot reach those of other permanent magnet materials such as Nd–Fe–B compounds. The crystallographic structure presents only one high-symmetry ($4/mmm$) site for the rare-earth ions.

The magnetic structure of these compounds is based on the existence of two magnetic sublattices, Fe and rare earth, either ferromagnetically or ferrimagnetically coupled through the 3d–4f exchange interaction. The competition between the magnetocrystalline anisotropy of the two sublattices can lead to the existence of spin reorientation transition (SRT) phenomena. The Fe sublattice anisotropy is assumed to be of 'easy-axis' type as in $YFe_{11}Ti$ (Moze *et al* 1988, Hu *et al* 1989). The sign of the second-order crystal-electric-field (CEF) gradient favours a contribution to the uniaxial anisotropy for the RE ions with second-order Stevens coefficient $\alpha_j > 0$ (i.e. RE = Sm, Er, Tm and Yb), therefore an SRT could be expected for the compounds with $\alpha_j < 0$ (RE = Nd, Tb, Dy and Ho). However, the observed anisotropic behaviour cannot be simply understood considering only the contribution of the second-order CEF terms to describe the RE magnetocrystalline anisotropy. The $ErFe_{11}Ti$

0953-8984/94/4810551+16$19.50

compound shows an SRT at $T_{SR} \approx 60$ K from the c axis to a non-collinear magnetic structure at low temperatures (Sinha *et al* 1989, Hu *et al* 1989, Kou *et al* 1993), although the Fe and second-order RE contributions favour the c axis as easy magnetization direction (EMD) in the entire range of temperatures. This fact may be considered as an indication of the relevance of high-order CEF terms to drive the SRT in these compounds.

In this paper we will focus our study on the $DyFe_{11}Ti$ intermetallic. This compound presents a complex magnetic behaviour with the existence of two SRTs in the ferrimagnetically ordered phase. The first SRT is of second order and takes place at $T_{SR1} \approx 200$–240 K (Boltich *et al* 1989, Hu *et al* 1990, Andreev *et al* 1990, Kou *et al* 1993). Below this temperature the magnetization rotates away from the room-temperature easy axis (c axis) to a conical non-collinear magnetic structure in which the EMD forms an angle θ with the c axis.

The second SRT occurs at a lower temperature, T_{SR2}, at which the EMD reaches the basal plane of the tetragonal structure. A wide range of values for T_{SR2} between 58 K and 120 K has been reported (Boltich *et al* 1989, Hu *et al* 1990, Andreev *et al* 1990, Kou *et al* 1993). Kou *et al* ascribed such discrepancies to the different values of the applied magnetic field. Moreover some controversy exists about whether the low-temperature SRT is a first- or second-order transition. Hu *et al* (1990) and Kou *et al* (1993) reported this low-temperature transition as a first-order transition. However Andreev *et al* (1990) interpreted their measurements as a second-order transition at T_{SR2} in which the magnetization does not reach the basal plane even at 4.2 K.

In a recent paper (García *et al* 1993) we carried out a study of the character of the low-temperature SRT. This study showed a dependence of the apparent character of the transition on the applied magnetic-field value.

A first-order magnetization process (FOMP) is shown by this compound under an applied magnetic field of the order of 10–20 kOe in the temperature range 4.2–100 K (Hu *et al* 1990, Andreev *et al* 1990).

The aim of this paper is to study the magnetic anisotropy of $DyFe_{11}Ti$, measuring the isothermal polar dependence of the parallel ($M_{\parallel}$) and perpendicular ($M_{\perp}$) components of the magnetization on the applied magnetic field (Del Moral *et al* 1988, Joven *et al* 1990). Due to the low value of the critical field at which the FOMP takes place, it has been possible to measure the polar dependence of $M_{\parallel}$ and $M_{\perp}$ at magnetic fields lower and higher than the reported critical field.

From our measurements the character of the second SRT will be clarified, under the assumption of the coexistence of two phases with different EMDs. The stability of these two phases is temperature and field dependent, which results in a continuous rotation of the effective average EMD.

A microscopic model that includes CEF and exchange interactions has been used in order to account for the thermal and field dependence of the EMD in the entire temperature range.

2. Experimental details

The $DyFe_{11}Ti$ single crystal was prepared by Song-Quan Ji at the Natuurkundig Laboratorium in Amsterdam using the Czochralski method in a triarc furnace. The sample was cut into two plates: one with its surface parallel to the $(\bar{1}10)$ plane and the other with its surface parallel to the (001) plane. The first of them allowed us to measure the anisotropy between the c axis and the easy direction in the basal plane (García *et al* 1993), and the second one to measure the anisotropy within the basal plane.

Measurements of the components of the magnetization parallel ($M_{\parallel}$) and perpendicular ($M_{\perp}$) to the applied magnetic field were performed using an extraction magnetometer within the temperature range of 4.2–300 K. The polar dependence of both components was obtained by rotating the sample in steady magnetic fields up to 20 kOe. $M_{\perp}$ is proportional to the torque that the sample experiences in the applied magnetic field and, consequently, reaches zero value when the magnetic field is applied along either the EMD or any major symmetry direction. The parallel component has a maximum when the magnetic field is applied along the EMD and a minimum at the hard directions. From these measurements it was possible to determine the EMD as a function of temperature and field with high accuracy.

3. Theoretical model

In the presence of an external magnetic field $\boldsymbol{H}$, the Hamiltonian describing the magnetic properties of the Dy^{3+} ion in the tetragonal $DyFe_{11}Ti$ compound can be written as

$$H = H_{\mathrm{CEF}} + g_{\mathrm{J}}\mu_{\mathrm{B}}\boldsymbol{J}\cdot\boldsymbol{H}_{\mathrm{mol}}(T) + g_{\mathrm{J}}\mu_{\mathrm{B}}\boldsymbol{J}\cdot\boldsymbol{H} \tag{1}$$

where H_{CEF} represents the CEF interaction on the rare-earth site, which in tetragonal symmetry and considering only the ground multiplet $|L, S, J, M_J\rangle$ of the Dy^{3+} ion, can be expressed as

$$H_{\mathrm{CEF}} = B_2^0 O_2^0 + B_4^0 O_4^0 + B_4^4 O_4^4 + B_6^0 O_6^0 + B_6^4 O_6^4 \tag{2}$$

where the B_n^m are the CEF parameters ($B_2^0 = 0.16$, $B_4^0 = -11 \times 10^{-4}$, $B_4^4 = 105 \times 10^{-4}$, $B_6^0 = -16 \times 10^{-6}$, $B_6^4 = -4 \times 10^{-6}$, in units of K/ion) (Hu *et al* 1990) and the O_n^m are the Stevens operators.

The second term of equation (1) is the exchange Hamiltonian, which represents the bilinear exchange interaction between the rare-earth and Fe magnetic sublattices and is considered within the molecular-field approximation. In the present model we assumed the RE–RE exchange interaction to be negligible and the Fe–Fe exchange interaction irrelevant in order to study the anisotropic behaviour. The thermal evolution of $\boldsymbol{H}_{\mathrm{mol}}$ (antiparallel to M_{Fe}) was obtained by using

$$\boldsymbol{H}_{\mathrm{mol}}(T) = -n_{\mathrm{REFe}}\gamma\rho\boldsymbol{M}_{\mathrm{Fe}}(T) \tag{3}$$

where n_{REFe} is the intersublattice exchange coefficient ($n_{\mathrm{REFe}} = 4\pi \times 141$, Hu *et al* 1990), $\gamma = 2(g_{\mathrm{J}} - 1)/g_{\mathrm{J}}$ and ρ (= 7.945 g cm^{-3}) is the density. The last term of equation (1) describes the Zeeman interaction of the Dy^{3+} sublattice under an applied magnetic field $\boldsymbol{H}$.

The free energy for the Dy^{3+} sublattice is obtained from the canonical partition function $Z = \sum_n \exp(-E_n/k_{\mathrm{B}}T)$ where E_n are eigenvalues of the Hamiltonian given by equation (1). The free energy $F^{\mathrm{RE}}(\theta, \phi, \theta_H, \phi_H, H, T)$ for the rare-earth sublattice is given by

$$F^{\mathrm{RE}}(\theta, \phi, \theta_H, \phi_H, H, T) = -(RT/M_{\mathrm{mol}})\ln Z \tag{4}$$

where H is the magnitude of the applied magnetic field, θ_H and ϕ_H are the standard spherical angles determining the direction of $\boldsymbol{H}$, θ and ϕ are the same angles for the molecular field, R is the gas constant and M_{mol} is the molecular mass.

The total free energy is calculated by adding on the uniaxial Fe sublattice anisotropy energy and also the Zeeman interaction for the Fe sublattice,

$$F(\theta,\phi,\theta_H,\phi_H,H,T) = F^{RE}(\theta,\phi,\theta_H,\phi_H,H,T) + K_1(T)\sin^2\theta - M_{Fe}(T)H[\sin\theta\sin\theta_H\cos(\phi_H-\phi)+\cos\theta\cos\theta_H] \quad (5)$$

where $M_{Fe}(T)$ and $K_1(T)$ are the magnetization and the anisotropy constant of the ion magnetic sublattice, taken from the $YFe_{11}Ti$ values (Hu *et al* 1989).

The magnetic structure at any given temperature and applied magnetic field is determined by the equilibrium angles θ_0 and ϕ_0 of the molecular field, which minimize the total free energy obtained from equation (5).

The magnetic moment of the Dy^{3+} ion is then calculated using the expression

$$m_i = -\frac{g_J\mu_B}{Z}\sum_n \langle n|J_i|n\rangle \exp\left(\frac{-E_n}{k_BT}\right) \qquad (i=x,y,z) \quad (6)$$

where E_n are the eigenvalues and $|n\rangle = \sum a_{nJ}|J,M_J\rangle$ the eigenvectors of the rare-earth Hamiltonian obtained from equation (1) for the equilibrium angles θ_0 and ϕ_0.

After calculation of the magnitude and direction of the magnetic moments of the Dy^{3+} ions and Fe magnetic sublattices it is possible to determine the components of the total magnetization parallel and perpendicular to the applied magnetic field. The component of the magnetization parallel to the field is given by

$$M_\parallel = M_{Fe}(T)[\sin\theta_H\sin\theta_0\cos(\phi_H-\phi_0)+\cos\theta_H\cos\theta_0] + m_x\sin\theta_H\cos\phi_H + m_y\sin\theta_H\sin\phi_H + m_z\cos\theta_H. \quad (7)$$

The component of the magnetization perpendicular to $\boldsymbol{H}$, when the magnetic field is applied in the $(\bar{1},1,0)$ plane, can be written as

$$M_\perp = (M_{Fe}(T)\cos\theta_0 + m_z)\sin\theta_H - \sqrt{2}(M_{Fe}(T)\sin\theta_0\cos\phi_0 + m_x)\cos\theta_H. \quad (8)$$

For $\boldsymbol{H}$ applied within the (001) plane (basal plane),

$$M_\perp = (M_{Fe}(T)\sin\theta_0\cos\phi_0 + m_x)\sin\theta_H - (M_{Fe}(T)\sin\theta_0\sin\phi_0 + m_y)\cos\theta_H. \quad (9)$$

Expressions (7), (8) and (9) allow us to determine $M_\parallel$ and $M_\perp$ in both single crystals used in the present work.

The former expressions are valid when the sample is a single domain. For low enough applied magnetic fields (in relation to the anisotropy field (Voigt and Pelster 1973)) and when the field direction lies near the hard magnetic direction the sample becomes multidomain and the theory should be modified to take into account the existence of magnetic domains. In fact when the magnetic field is applied along a hard direction the sample decomposes into equivolume domains, the magnetization in those domains is symmetrical with respect to the field direction and the torque is zero.

For temperatures below T_{SR2} the hard magnetic direction (HMD) is the tetragonal c axis [001] and the EMD is the [110] direction. For $T_{SR2} < T < T_{SR1}$ the c axis and the [110] direction in the basal plane are HMDs. For $T < T_{SR1}$, when the magnetic field is applied along the c axis, four domains will exist and two situations are possible: (i) for $T < T_{SR2}$, the magnetization of the domains is along the [110], $[1\bar{1}0]$, $[\bar{1}\bar{1}0]$, $[\bar{1}10]$ directions, and (ii)

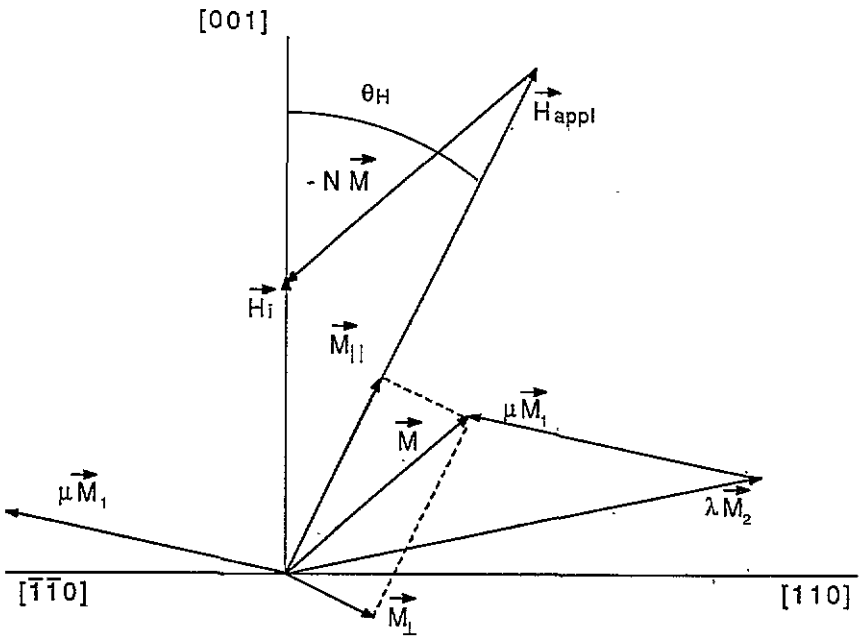

Figure 1. A schematic representation of the magnetic moments and magnetic fields in the two-domain regime, within the $(\bar{1}, 1, 0)$ plane.

for $T_{SR2} < T < T_{SR1}$, the magnetization makes an angle θ_0 with the c axis, lying in the four planes defined by the [001] and the [110], [1$\bar{1}$0], [$\bar{1}\bar{1}$0], [$\bar{1}$10] directions. The sample used in the present work, containing the [001] axis, was cut with the surface parallel to the ($\bar{1}$10) plane and the magnetic field was applied in that plane, thus the domains with the magnetization in the ($\bar{1}$10) plane are favoured. Therefore, we consider that when the magnetic field is applied away from an HMD and makes an angle θ_H with the c axis, only two domains, with magnetization M_1 and M_2 respectively, lying in the plane containing [001] and the applied magnetic field direction, will remain (figure 1).

Both domains should have the same energy and coexist in equilibrium under the presence of the applied magnetic field (Néel *et al* 1960). This equilibrium is possible when the total magnetization M originates an internal field H_i along the HMD (see figure 1). The spontaneous magnetization within both domains (M_1 and M_2) is symmetrical with respect to the HMD. The relative volumes λ and μ of these domains change by the wall-displacement mechanism as the magnetic field rotates.

Assuming the volume of the sample equal to unity and the c axis as the HMD, the relative volume fraction of both domains (λ and μ) can be calculated from the following equations (Barnier *et al* 1962):

$$\lambda = \tfrac{1}{2}(1 + (H \sin\theta_H)/NM \sin\theta_0) \qquad \mu = \tfrac{1}{2}(1 - (H \sin\theta_H)/NM \sin\theta_0) \tag{10}$$

where $N(= 4\pi \times 0.24)$ is the experimental demagnetizing factor taken from the slope, at $H \to 0$, of the experimental $M(H)$ isotherm at 4.2 K when the field is applied along the [$\bar{1}$10] direction.

In equation (10) N, H and θ_H are known from the experimental conditions and M and θ_0 can be calculated using the microscopic single-ion model. Therefore we can theoretically

calculate the relative volume fraction of both domains in each experimental situation and the two-domain structure will exist while $\mu, \lambda < 1$.

Under such a hypothesis $M_{\parallel}$ can be obtained as

$$M_{\parallel} = M_y \sin\theta_H \sin\phi_H + M_z \cos\theta_H + (\lambda - \mu) M_x \sin\theta_H \cos\phi_H \tag{11}$$

where M_i is the total magnetization component (Fe and rare-earth sublattices) along the i axis ($i = x, y, z$). $M_{\perp}$ is

$$M_{\perp} = M_z \sin\theta_H + (\mu - \lambda)\sqrt{2} M_x \cos\theta_H. \tag{12}$$

Expression (11) and (12) will become relevant in order to explain the experimental results at low magnetic field applied near the c axis.

In the conical regime ($T_{SR2} < T < T_{SR1}$) a multidomain structure will also exist when the magnetic field is applied near the basal plane, but the angular region around $\theta_H = \pi/2$ in which the four domains exist is very narrow and no multidomain correction for domains is necessary (see subsection 4.2).

4. Results and discussion

4.1. The $(\bar{1}, 1, 0)$ plane

4.1.1. Low-field behaviour ($H < 5$ kOe). Experimental measurements of the polar dependence of $M_{\parallel}$ and $M_{\perp}$ have been performed in the temperature range between 4.2 and 300 K for applied magnetic fields lower than the critical FOMP fields. In figure 2 we present the experimental results obtained in the spin-reorientation region ($T < T_{SR1}$) together with the theoretical calculations using the model described above. In this field range ($H \leqslant 5$ kOe) the above two-domain model should be applied. We have used the CEF and exchange parameters given by Hu *et al* (1990) (the signs of B_4^4 and B_6^4 CEF parameters were changed to take into account that the easy direction in the basal plane is [110] rather than [100]) (Garcia *et al* 1993).

At the lower temperatures (4.2 K and 25 K) the EMD lies in the basal plane and the parallel magnetization shows a maximum at $\theta = 90°$. The agreement between the experimental results and the theoretical predictions is good even when the magnetic field lies in a direction close to the HMD, a situation in which the two-domain approximation acquires special relevance.

In the temperature range between 75 K and 150 K the system remains conical (figure 2(*d*)–(*f*)) with angles of 39°, 38° and 28° for $T = 75$, 100 and 150 K respectively and the agreement between the experimental and theoretical results is quite good in the entire temperature range. At $T = 75$ K, in the conical magnetic-structure region, we applied the multidomain approach only when such correction was important, i.e. when the magnetic field was applied near the c axis. For magnetic fields near the HMD in the basal plane the multidomain region is narrow (see figures 2(*d*)–(*f*)) and no correction was made.

At $T = 200$ K the system is an easy-axis magnet having a maximum for the parallel component of the magnetization at $\theta = 0°$ (see figure 2(*g*)).

At $T = 50$ K (figure 2(*c*)) a disagreement between the experimental and theoretical results is evident even considering the two-domain approach. $M_{\parallel}$ presents a maximum and $M_{\perp}$ reaches a zero value at an intermediate direction between the c axis and the basal plane ($\theta = 69°$) indicating that the macroscopic EMD lies along a non-major symmetry direction.

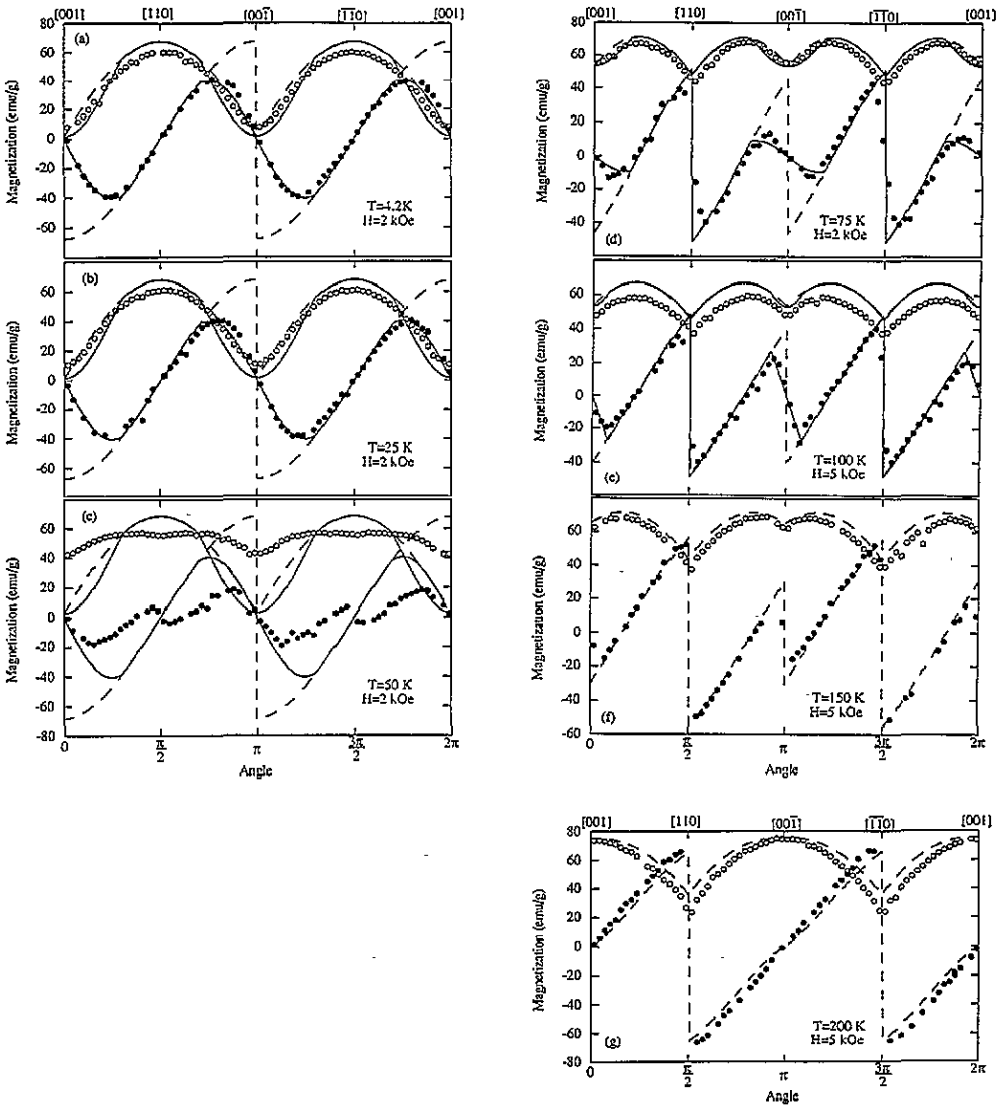

Figure 2. The angular dependence of the parallel (○) and perpendicular (●) components of the magnetization in the ($\bar{1}$, 1, 0) plane at some selected temperatures: (*a*) $T = 4.2$ K, (*b*) $T = 25$ K, (*c*) $T = 50$ K, (*d*) $T = 75$ K, (*e*) $T = 100$ K, (*f*) $T = 150$ K, (*g*) $T = 200$ K. The lines are theoretical calculations considering the monodomain approach (– – –) and the two-domain theory (——).

In order to test the value obtained for the EMD angle from the polar $M_{\parallel}$ and $M_{\perp}$ measurements, we also performed measurements of the thermal dependence of the magnetization along the [001] and [110] axes in the temperature range of 4.2–250 K, using a steady magnetic field of 2 kOe. From these experimental results it is possible to estimate the EMD angle in a simple way

$$\theta = \tan^{-1}(M_{[110]}/M_{[001]}). \tag{13}$$

In figure 3 we present the experimental results obtained in this way as well as the

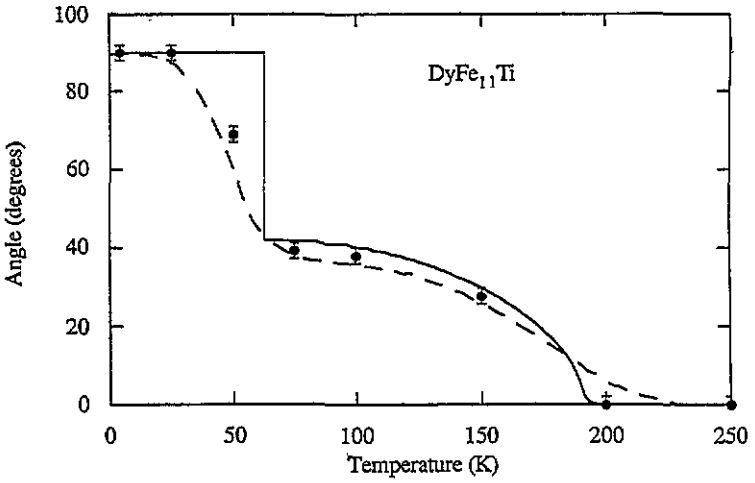

Figure 3. The thermal dependence of the spin reorientation angle for $DyFe_{11}Ti$, obtained from polar measurements of $M_{\parallel}$ and $M_{\perp}$ (●) and from measurement of the magnetization along the [100] and [110] directions with an applied magnetic field of 2 kOe (– – –). The continuous line is the theoretical SRT angle using the CEF and exchange parameters given by Hu *et al* (1990).

experimental value obtained from measurements of the polar dependence of $M_{\parallel}$ and $M_{\perp}$ and also the theoretical fit using the CEF and exchange parameters given by Hu *et al* (1990). An excellent agreement between the two determinations of the EMD is observed, showing a continuous rotation of the macroscopic EMD between the easy-plane phase and the easy-axis phase.

The agreement between the experimental and theoretical results is good for temperatures higher than the theoretical T_{SR2} (= 60 K) and for $T < 25$ K, but in the intermediate-temperature region (25 K $< T <$ 60 K) the agreement is poor: the theory predicts an easy-plane region and the experiment shows an easy-cone magnetic structure (see figure 3).

To explain such a discrepancy we will consider that in the intermediate-temperature region the sample consists of two magnetic phases corresponding to the low-temperature ($T < 25$ K) planar phase (PP), with $\theta = 90°$, and high-temperature ($T > 60$ K) conical phase (CP), with $\theta \approx 40°$. In the intermediate region the two phases coexist with different relative volumes depending on the temperature and the magnetic field. As a consequence, an apparent EMD, intermediate between the conical and planar structures, can be expected for such a temperature region as has been observed at $T = 50$ K.

The presence of the two phases in the sample can be related to the existence of two minima, theoretically predicted, in the total free energy at $\theta \approx 40°$ and $\theta = 90°$ (Hu *et al* 1990). For $T > T_{SR2}$ the absolute minimum corresponds to a conical phase. As the temperature decreases, the planar phase grows inside the domain walls present in the conical phase. This process will finish at $T \approx 25$ K; below this temperature the only phase present will be the low-temperature PP.

In order to confirm this hypothesis we fitted the experimental results of $M_{\parallel}$ and $M_{\perp}$ observed at $T = 50$ K, assuming that the PP and CP are represented by the experimental curves obtained at $T = 25$ K (PP) and $T = 75$ K (CP) (see figure 2(*b*) and (*d*)). Under such an assumption we can write

$$M_{\parallel}(50\text{ K}) = xM_{\parallel}(25\text{ K}) + (1-x)M_{\parallel}(75\text{ K}) \tag{14a}$$

$$M_{\perp}(50\ \mathrm{K}) = xM_{\perp}(25\ \mathrm{K}) + (1-x)M_{\perp}(75\ \mathrm{K}) \qquad (14b)$$

where x is the relative volume of the PP. The result for $x = 0.5$ is shown in figure 4: a good agreement has been obtained, supporting our previous assumption of coexistence of two magnetic phases in the sample in the intermediate-temperature region, whilst with the single-phase model it was impossible to interpret the data (see figure 2(*c*)).

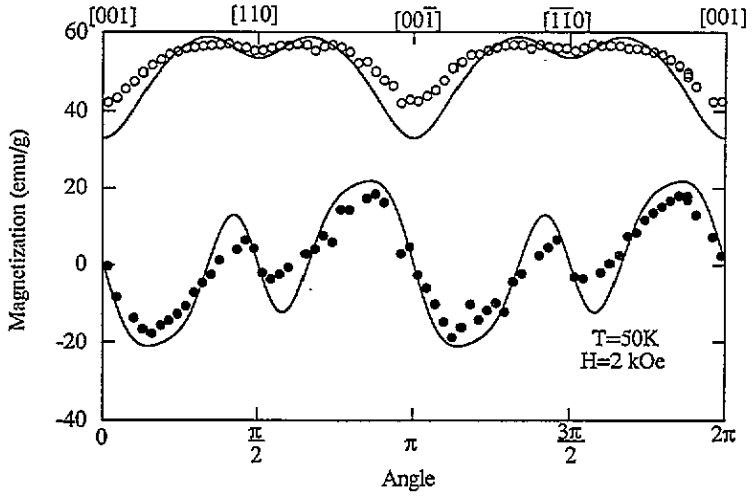

Figure 4. A fit of the angular dependence of $M_{\parallel}$ and $M_{\perp}$ at $T = 50$ K using equations (14*a*) and (14*b*) for $x = 0.5$ (see the text for details).

4.1.2. Magnetic-field behaviour of $M_{\parallel}$ and $M_{\perp}$ ($H > 2$ kOe). The study of the magnetic-field dependence of the polar plots is especially important when a FOMP takes place at a certain critical field (H_{cr}). This kind of phenomenon occurs in $DyFe_{11}Ti$, as can be observed in the magnetization isotherm of figure 5, when a magnetic field is applied along the [001] direction. We have measured the polar dependence of $M_{\parallel}$ and $M_{\perp}$ at different field and temperature values. As an example we present in figure 6 the results obtained at 4.2 K for several applied magnetic fields lower and higher than the internal critical field ($H_{cr} \approx 5$ kOe, Hu *et al* 1990).

The result obtained for $H < H_{cr}$ has been already presented in figure 2(*a*), showing a typical easy-plane behaviour.

For $H > H_{cr}$ (figure 6(*a*) and (*b*)) the shape of the polar dependence of $M_{\parallel}(\theta_H)$ and $M_{\perp}(\theta_H)$ drastically changes; new maxima appear in $M_{\parallel}$ and jumps in $M_{\perp}$ are induced by the magnetic field at certain non-major symmetry directions. This behaviour can be understood under the assumption of the existence of a critical angle for the applied magnetic field. At this temperature the system has two minima in the total free energy (Hu *et al* 1990) and consequently a first-order magnetic transition induced by the magnetic field can be expected. In a standard isotherm the magnetic-field direction is constant and the strength of the magnetic field is changed. For a critical value of the field strength a FOMP takes place, giving rise to an increase of the magnetization parallel to the applied magnetic field.

In our measurements the magnetic-field strength is constant and its direction is changed. Now instead of H_{cr} we will obtain a critical angle (formed by the applied magnetic field and

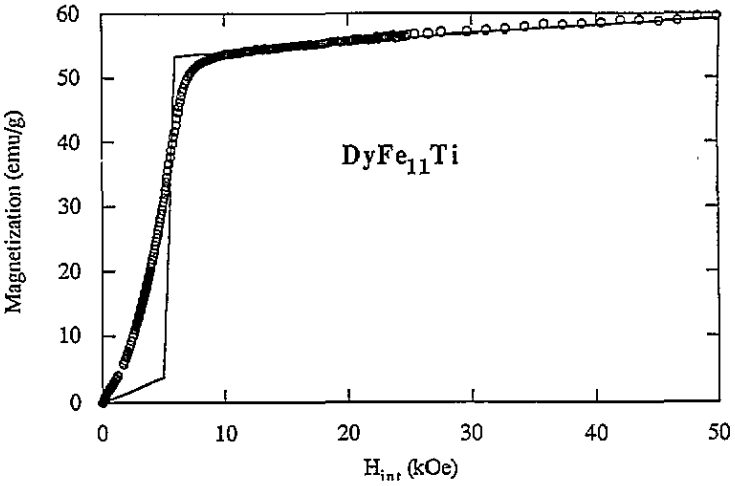

Figure 5. Experimental (O) and calculated (——) magnetization curves at $T = 4.2$ K for H along the c axis.

the c axis, θ_H^{cr}) at which the magnetization jumps between the directions in which the free energy presents both minima. Such is the process observed in the experimental results. The strength of the applied magnetic field gives rise to an internal magnetic field higher than H_{cr}. Therefore, when the field is applied along the [001] direction the EMD is defined by the absolute minimum of the total free energy at $\theta \approx 40°$. Rotating the magnetic field towards that direction an increase of $M_\parallel$ and a decrease of $|M_\perp|$ is observed (see figure 6(a)). By rotating the magnetic field towards the basal plane, the minimum of the total free energy in the basal plane is favoured, and for a certain θ_H^{cr} the absolute minimum of the free energy is changed to $\theta \approx 90°$. At this θ_H^{cr} value a decrease of $M_\parallel$ and an increase of $|M_\perp|$ is observed (see figure 6(a)).

When $H \approx H_{cr}$ (figure 6(c)) the $M_\parallel(\theta_H)$ and $M_\perp(\theta_H)$ results display essentially an easy-plane behaviour with a maximum in $M_\parallel$ when the magnetic field is applied along the [110] direction. An additional small maximum starts to appear near the hard direction (the c axis). A poor agreement between the experimental and the theoretical results has been obtained in this applied-magnetic-field region at low temperatures (see figure 6(a)).

A similar behaviour has been obtained on the isotherm magnetization results (Hu *et al* 1990, García *et al* 1993) (see figure 5) in which a continuous increase of the magnetization instead of a jump is observed at $H \approx 5$ kOe. As in the case of the spin reorientation angle, we will suppose that, in the magnetic field range near H_{cr}, this continuous variation of the magnetization can be ascribed to the coexistence of a low-field (LF) PP (with $\theta \approx 90°$) and a high-field (HF) CP (with $\theta \approx 40°$). We will ascribe the LF and the HF behaviour at 4.2 K to the previous reported polar-dependence results at $H = 2$ kOe (figure 2(a)) and $H = 15$ kOe (figure 6(a)). Therefore we have fitted the experimental results at $H = 5$ kOe using

$$M_\parallel(5\text{ kOe}) = xM_\parallel(2\text{ kOe}) + (1-x)M_\parallel(15\text{ kOe}) \tag{15a}$$

$$M_\perp(5\text{ kOe}) = xM_\perp(2\text{ kOe}) + (1-x)M_\perp(15\text{ kOe}). \tag{15b}$$

The result obtained for the best fit, obtained at $x = 0.4$, is presented in figure 7(a), showing a good agreement, supporting again our previous hypothesis of the coexistence of two phases.

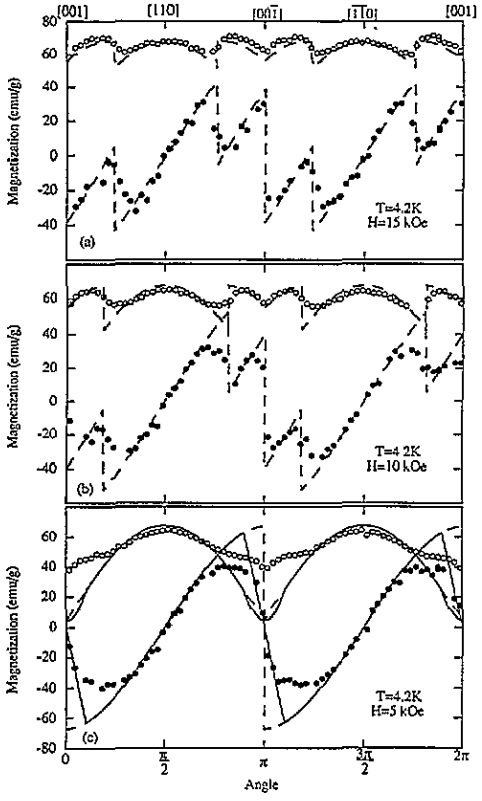

Figure 6. The angular dependence of the parallel (○) and perpendicular (●) components of the magnetization within the $(\bar{1}, 1, 0)$ plane at $T = 4.2$ K and at some selected magnetic fields: (*a*) $H = 15$ kOe; (*b*) $H = 10$ kOe; (*c*) $H = 5$ kOe. The lines are theoretical calculations considering the monodomain approach (– – –) and the two-domain theory (——).

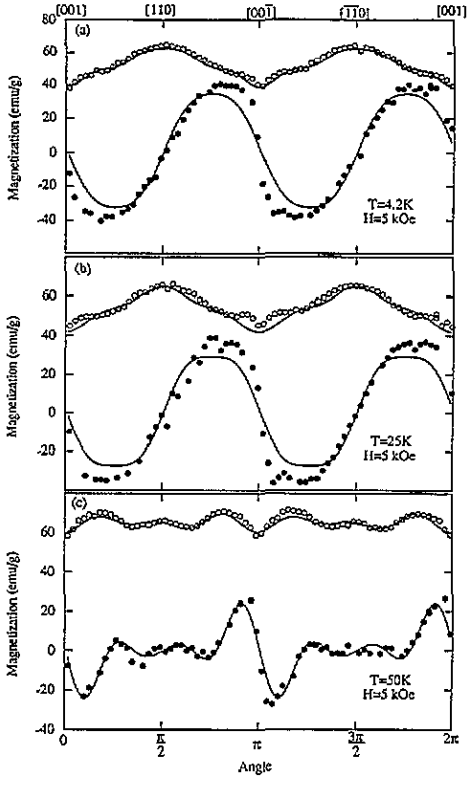

Figure 7. The angular dependence of the parallel (○) and perpendicular (●) components of the magnetization within the $(\bar{1}, 1, 0)$ plane at $H = 5$ kOe and at the following temperatures: (*a*) $T = 4.2$ K; (*b*) $T = 25$ K; (*c*) $T = 50$ K. The lines are the fits using equations (15*a*) and (15*b*) for (*a*) $x = 0.4$, (*b*) $x = 0.4$ and (*c*) $x = 0.25$ (see the text for details).

A similar behaviour is shown by the experimental results for $T = 25$ and 50 K at $H \approx H_{cr}$. We have fitted the experimental results using equations (15*a*) and (15*b*) and the results are shown in figure 7(*b*) and (*c*), respectively.

4.2. The (001) plane

A high anisotropy in the (001) plane between the [110] and [100] directions has been reported by Hu *et al* (1990) from magnetization measurements. This anisotropy is large even at room temperature and increases as temperature is lowered. Also a study on the isomorphous $REFe_{10}V_2$ compounds (Algarabel *et al* 1992) revealed a high basal-plane anisotropy up to near room temperature.

In this section we report a study of the magnetic anisotropy in the basal plane measuring the polar dependence of $M_{\parallel}$ and $M_{\perp}$. In figure 8 we present the experimental results obtained at some selected temperatures under an applied magnetic field of 15 kOe. At this value of the applied magnetic field the sample is monodomain for any direction of the applied magnetic field in the basal plane.

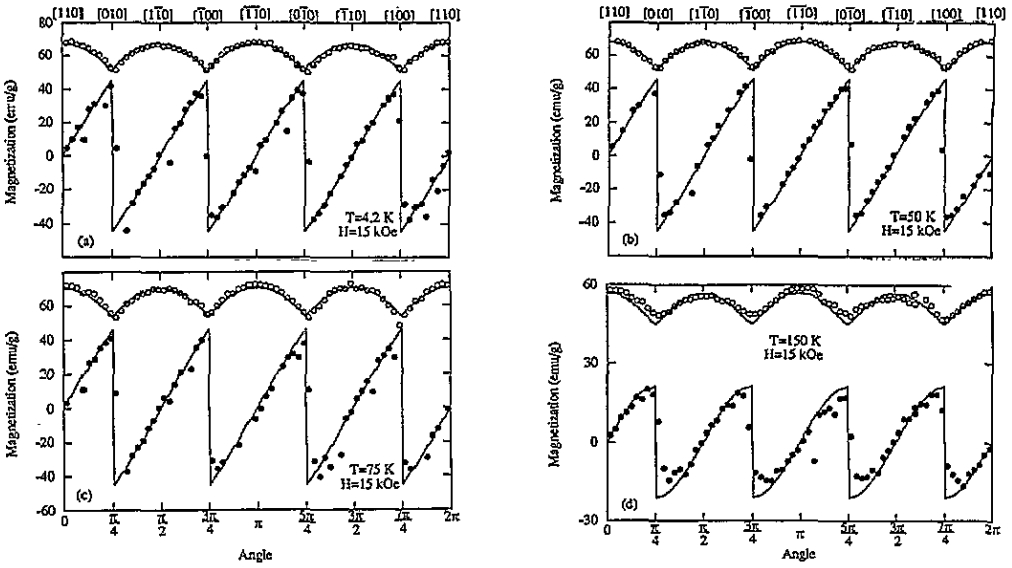

Figure 8. The angular dependence of the parallel (O) and perpendicular (●) components of the magnetization within the basal plane at some selected temperatures: (*a*) $T = 4.2$ K; (*b*) $T = 50$ K; (*c*) $T = 75$ K; (*d*) $T = 150$ K. The lines are theoretical calculations considering the monodomain approach (——).

The results show a 90° periodicity as corresponds to a system with tetragonal symmetry in the basal plane. The EMD, determined by the maximum of $M_{\parallel}$ and $M_{\perp} = 0$, remains along the [110] direction in the whole temperature range. The study of the polar dependence was performed at several values of applied magnetic field, but in this plane we did not observe any experimental evidence of a FOMP at $H \leqslant 20$ kOe.

In order to explain the magnetic behaviour within the basal plane we have used the model described in section 3. In figure 8 it is possible to observe the excellent explanation of our experimental results using this microscopic model.

4.3. The temperature and field dependence of the relative volume of the PP and CP magnetic phases

From the polar dependence of $M_{\parallel}$ and $M_{\perp}$ reported in the previous section, the coexistence of two magnetic phases at temperatures near the low-temperature spin reorientation and for applied magnetic fields near the critical FOMP field is clearly evidenced.

In order to determine the relative volume fraction of both magnetic phases in this coexistence region, as a function of temperature and the applied magnetic field, we have measured the magnetization as a function of temperature along the [001], $M_{[001]}$, and the [110], $M_{[110]}$, directions under an applied field of 2 kOe and the magnetization as a function of the field along the [001] direction at 4.2 K.

From our experimental results a continuous variation of $M_{[001]}(T)$ and $M_{[110]}(T)$ at both SRTs is clearly shown (see figure 9). This result is in agreement with a second-order SRT at $T_{SR1} \approx 200$ K. However, in the low temperature SRT, where a first-order transition takes place, the continuous variation may be related to the coexistence of the two magnetic phases. We can assume, looking at the experimental results, that this coexistence may be extended in a range of temperatures around the SRT, going from 20 K to 80 K. Our hypothesis is based on the consideration that at temperatures below 20 K only the PP exists

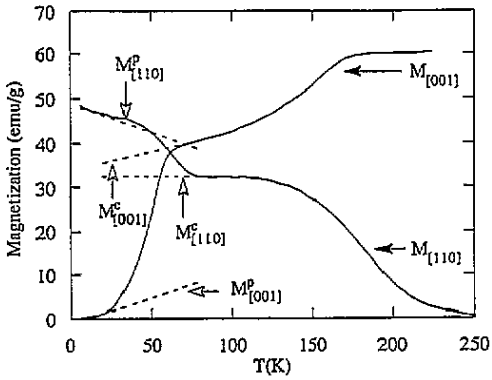

Figure 9. The thermal dependence of the magnetization along the [001], $M_{[001]}$, and [110], $M_{[110]}$, axes under an applied field at 2 kOe. The lines (– – –) are the extrapolation from the PP and CP to the two-phase region.

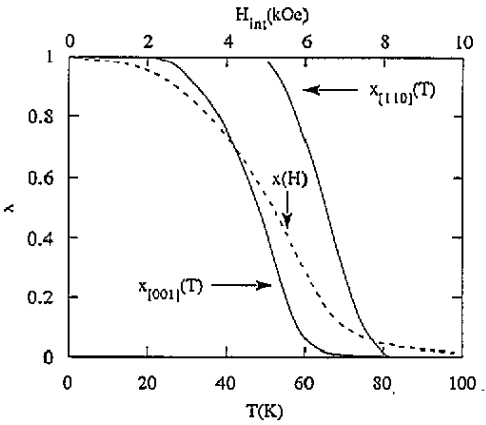

Figure 10. The thermal and field dependence of the relative volume of the PP in the two-phase region for the different experimental situations studied (see the details in the text).

and at temperatures above 80 K only the CP does. We have proceeded to fit the thermal dependence of the magnetization in the CP and PP near T_{SR2} to straight lines and these functions were extrapolated to the intermediate-temperature range (from 20 K to 80 K). These fits are shown in figure 9, where we denoted the fitting functions as $M^P_{[001]}(T)$ and $M^P_{[110]}(T)$ at temperatures at which only the PP is supposed to exist, and $M^C_{[001]}(T)$ and $M^C_{[110]}(T)$ at temperatures at which only the CP is supposed to exist. Thus, the experimental magnetization, in the intermediate-temperature range at which both magnetic phases coexist, can be written, in a way similar to equations (14*a*) and (14*b*),

$$M_{[001]}(T) = x_{[001]}M^P_{[001]}(T) + (1 - x_{[001]})M^C_{[001]}(T) \tag{16a}$$

$$M_{[110]}(T) = x_{[110]}M^P_{[110]}(T) + (1 - x_{[110]})M^C_{[110]}(T) \tag{16b}$$

where $x_{[001]}$ and $x_{[110]}$ are the relative volume fractions determined with the magnetic field applied along the [001] and the [110] directions, respectively. From the expressions (16*a*) and (16*b*) $x_{[001]}$ and $x_{[110]}$ are easily obtained and these two quantities are shown in figure 10. An anisotropy of $x(T)$ with the direction of the applied field is evident. This result should be expected because the direction of the applied field favours or inhibits the CP as seen in the polar-plot measurements. The range of temperature in which the two phases coexist extends around 40 K.

To determine the dependence of x on the applied magnetic field, measurements of the magnetization as a function of the magnetic field applied along the [001] direction at 4.2 K were made. For this purpose, the sample had been specially shaped as an ellipsoid with a small demagnetization factor $N_z = 4\pi \times 0.047$. In figure 11, the magnetization against the internal field is presented. From the experimental results a continuous variation of magnetization is evident, while a FOMP transition should be expected from the theoretical calculation. We can understand this fact taking into account, again, the coexistence of the two phases under the applied field. We can consider that at fields lower than 1 kOe only the PP exists and at fields higher than 10 kOe only the CP does. We fitted the

experimental magnetization in these two regions to straight lines, denoted as $M^{P}(H)$ and $M^{C}(H)$ respectively, which were extrapolated into the intermediate-field region as shown in figure 11. As a consequence we can consider that the experimental $M(H)$ in the intermediate fields, where the two phases coexist, is given by

$$M(H) = xM^{P}(H) + (1-x)M^{C}(H). \tag{17}$$

The field dependence of x is shown in figure 10, where the coexistence of the two phases is extended to an interval of about 6 kOe around the critical FOMP field, $H_C \approx 5$ kOe.

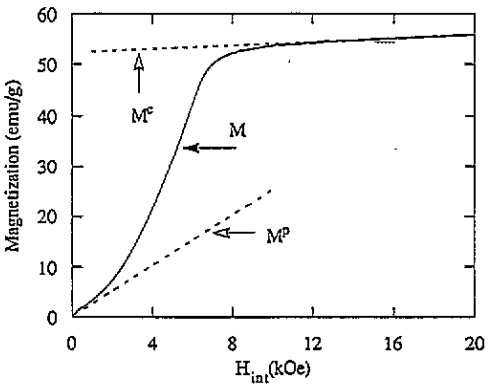

Figure 11. The magnetization isotherm at $T = 4.2$ K with H applied along the [001] axis. The lines (– – –) are the extrapolation from the PP and CP to the two-phase region.

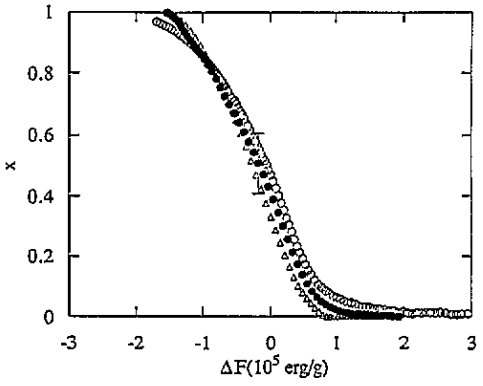

Figure 12. The relative volume, x, of the PP against ΔF for the different situations studied: Δ, $x(H)$; ●, $x_{[001]}(T)$ and ○, $x_{[110]}(T)$ (see the details in the text). From the slopes of these curves the Γ parameter has been obtained.

With allowance for coexistence of two phases, the free energy can be written as (Swalin 1962)

$$F = xF^{P} + (1-x)F^{C} + \tfrac{1}{2}\Gamma x(1-x) \tag{18}$$

where F^{C} is the free energy in the conical phase, and F^{P} that in the planar one. The third term reflects the existence of long-range interaction between the two phases. When $\Gamma > 0$, the free energy has a minimum at

$$x = \tfrac{1}{2} + \Delta F/\Gamma \tag{19}$$

where $\Delta F = F^{C} - F^{P}$, and the two-phase system is stable in a temperature and field region for which $0 < x < 1$. Since both F^{C} and F^{P} depend on T and H, x will depend on both parameters. From the model of section 3 we calculated F for $\theta_H = 0°$ and $\phi_H = 45°$, with $H = 2$ kOe and temperatures ranging from 4 to 100 K. At each temperature we determined the angular dependence $F(\theta)$, with θ within the (1,1,0) plane. Two minima were found, one at $\theta \approx 90°$, which corresponds to the PP, and the other at $\theta \approx 40°$, as corresponds to the CP. Then, we assumed that $F^{C}(T) = F_{min}(\theta \approx 40°, T)$ and $F^{P}(T) = F_{min}(\theta \approx 90°, T)$ and calculated $\Delta F(T)$. A similar procedure was carried out for fixed $T = 4.2$ K and the field varying between $H = 0$ and 50 kOe. Again two minima were found, and assuming that $F^{C}(H) = F_{min}(\theta \approx 40°, H)$ and $F^{P}(H) = F_{min}(\theta \approx 90°, H)$ we calculated $\Delta F(H)$.

We have determined experimentally $x_{[110]}(T)$ and $x_{[001]}(T)$ for $H = 2$ kOe and $x(H)$ for $T = 4.2$ K, and we have calculated $\Delta F(T, H)$ so we can plot three independent *x versus* ΔF curves, eliminating T or H (figure 12). It is very interesting to see that the three curves are very similar in spite of their very different experimental conditions. Such a similarity allows us to be more confident in the validity of the simple interaction model. In fact, in the simplest model Γ can be considered as a constant and it can be determined from the slope of the $x(\Delta F)$ curve in figure 12. The value obtained in this way is $\Gamma = (2 \pm 0.3) \times 10^5$ erg g^{-1}.

The most probable mechanism responsible for such long-range interaction is magnetodipolar. The corresponding contribution to the free energy, i.e. magnetostatic energy, can be expressed as

$$F_{\text{dip}} = \tfrac{1}{2} N \rho \langle M \rangle^2 \tag{20}$$

where N is the demagnetization factor and $\langle M \rangle$ is the average magnetization (per volume unit). This macroscopic average can be expressed as $\langle M \rangle = x M^{\text{C}} + (1 - x) M^{\text{P}}$ where x is the volume fraction of the CP. Substituting (17) in expression (20) and comparing with (18), one may identify Γ with $N\rho(M^{\text{C}} - M^{\text{P}})^2$. Since we know from experiment the values for $M^{\text{C}} - M^{\text{P}} = 45 \pm 5$ emu g^{-1} (figure 11), we may derive the apparent demagnetization factor, obtaining

$$N = 4\pi \times 0.95 \pm 0.1.$$

This value is unexpectedly high, although not unreasonable. In the two-phase region the system seems to behave as if the domains of CP were isolated plates perpendicular to [001]; in such a case one would have $N_{001} \sim 4\pi$ rather than $N_{001} = 4\pi \times 0.047$ as dictated by the shape of the sample. This conjecture calls for a careful study of the domain structure in the low-temperature region, which is currently under way.

5. Conclusions

The measurements of the angular dependence of $M_{\parallel}$ and $M_{\perp}$ performed on a single crystal of $DyFe_{11}Ti$ have provided a more detailed description of the interplay between the basic interactions in this compound. The single-ion mean-field microscopic model used can account for the thermal, field and angular dependence of the magnetization components. In order to explain the obtained angular dependence of $M_{\parallel}$ and $M_{\perp}$, a two-domain model was used. This correction was relevant when the magnetic field was applied along a direction close to the HMD.

The present experiments have clarified the existing controversy about the low-temperature SRT (plane–cone). It has been definitively established to be a first-order phase transition.

The theoretical prediction reveals at low temperature the existence of two minima in the free energy, corresponding to two states in which the EMD lies along different directions. The ground state at low temperature and low field represents the PP. The CP constitutes a metastable state, which can be reached either by rising temperature or by application of magnetic field along the c axis. Consequently, the SRT is a first-order transition. However no discontinuities can be observed in the thermal and field dependences of $M_{\parallel}$, $M_{\perp}$ and θ. We have explained this behaviour considering a coexistence of PP and CP over a range of temperature and magnetic fields. Estimation of the volume fraction of both phases in the coexistence intervals has been performed.

Acknowledgments

We acknowledge the assistance and help in numerical calculation of Mr L Morellon who provided the starting programs and Professor J M D Coey for the provision of the single-crystalline specimens. This research has been partially supported by the Spanish DGICYT through the grants PB92-0095 and MAT93-0240-C04-04 and by the European Community under the project BREU-68-C and the CEAM III project. MDK acknowledges the MEC of Spain for the grant SB93-AOKIII150.

References

Algarabel P A, Pareti L, Marquina C, Solzi M, Ibarra M R and Marusi G 1992 *J. Appl. Phys.* **71** 366

Andreev A V, Bartashevich M I, Kudrevatykh N V, Razgonyaev S M, Sigaev S S and Tarasov E N 1990 *Physica* B **167** 139

Barnier Y, Pauthenet R and Rimet G 1962 *Cobalt* **15** 14

Boltich E B, Ma B M, Zhang L Y, Pourarian F, Malik S K, Sankar S G and Wallace W E 1989 *J. Magn. Magn. Mater.* **78** 364

Buschow K H J, de Mooij D B, Mitchell I V, Coey J M D, Givord D, Harris I R and Hanitsch R 1989 *Concerted European Action on Magnets* ed I V Mitchell, J M D Coey, D Givord, I R Harris and R Hanitsch (London: Elsevier)

Del Moral A, Joven E, Ibarra M R, Arnaudas J I, Abell J S and Algarabel P A 1988 *J. Physique Coll.* 49 C8 449

Franse J M M and Radwanski R 1992 *Handbook of Magnetic Materials* vol 7, ed K H J Buschow (Amsterdam: North-Holland) ch 5

García L M, Bartolomé J, Algarabel P A, Ibarra M R and Kuz'min M D 1993 *J. Appl. Phys.* **73** 5908

Hu B P, Li H S, Coey J M D and Gavigan J P 1990 *Phys. Rev.* B **41** 2221

Hu B P, Li H S, Gavigan J P and Coey J M D 1989 *J. Phys. C: Solid State Phys.* **1** 755

Joven E, del Moral A and Arnaudas J I 1990 *J. Magn. Magn. Mater.* **83** 558

Kou X C, Zhao T S, Grossinger R, Kirchmayr H R, Li X and de Boer F R 1993 *Phys. Rev.* B **47** 3231

Li H S and Coey J M D 1991 *Handbook of Magnetic Materials* vol 6, ed K H J Buschow (Amsterdam: North-Holland) ch 1

Moze O, Pareti L, Solzi M and David W I F 1988 *Solid State Commun.* **66** 465

Néel L, Pauthenet R, Rimet G and Giron V S 1960 *J. Appl. Phys.* **31** 27S

Sinha V K, Malik S K, Adroja D T, Elbicki J and Wallace W E 1989 *J. Magn. Magn. Mater.* **80** 281

Swalin R A 1962 *Thermodynamics of Solids* (New York: Wiley)

Voigt C and Pelster H H 1973 *Phys. Status Solidi* a **17** K97